

Structural Revision and Elucidation of the Biosynthesis of Hypodoratoxide by ^{13}C , ^{13}C COSY NMR Spectroscopy

Lena Barra, Kerstin Ibrom, and Jeroen S. Dickschat*

Abstract: Feeding of (2,3,4,5,6- $^{13}\text{C}_5$)mevalonolactone to the fungus *Hypomyces odoratus* resulted in a completely labeled sesquiterpene ether. The connectivity of the carbon atoms was easily deduced from a ^{13}C , ^{13}C COSY spectrum, revealing a structure that was different from the previously reported structure of hypodoratoxide, even though the reported ^{13}C NMR data matched. A structural revision of hypodoratoxide is thus presented. Its absolute configuration was tentatively assigned from its co-metabolite *cis*-dihydroagarofuran. Its biosynthesis was investigated by feeding of (3- ^{13}C)- and (4,6- $^{13}\text{C}_2$)mevalonolactone, which gave insights into the complex rearrangement of the carbon skeleton during terpene cyclization by analysis of the ^{13}C , ^{13}C couplings.

The mountaintop of molecular diversity within secondary metabolites is represented by the more than 50000 known terpenes from all kingdoms of life. Their biosynthesis involves complex reactions that are usually catalyzed by a single terpene cyclase, which converts a linear precursor, such as geranyl diphosphate (GPP), farnesyl diphosphate (FPP), or geranylgeranyl diphosphate (GGPP), into a terpene hydrocarbon or alcohol. This conversion proceeds via cationic intermediates in a domino reaction with several elementary steps, such as cyclizations, hydride and proton shifts, Wagner–Meerwein rearrangements, and fragmentations, resulting in (poly)cyclic frameworks with several stereogenic centers.^[1] The initial product can be modified by oxygenases or acyl transferases, for example, to generate a highly functionalized terpenoid. The structural complexity of terpenoids renders their structure elucidation difficult, and although structural data of terpene cyclases have contributed significantly to our understanding of terpene biosynthesis,^[2–9] it is challenging to gain insights into the intricate mechanisms of terpene cyclizations. Herein, we present an approach that addresses both problems by feeding of ^{13}C -labeled precursors and ^{13}C , ^{13}C correlation spectroscopy (COSY).

In our continued research program on the biosynthesis of bacterial and fungal terpenes, we noticed that the production of one major sesquiterpene **1** by the fungus *Hypomyces*

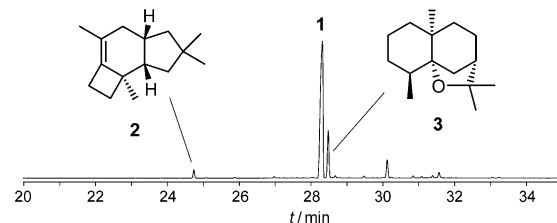


Figure 1. Total ion chromatogram of a headspace extract from *Hypomyces odoratus* DSM 11934.

odoratus DSM 11934 was accompanied by traces of other sesquiterpenes (Figure 1). Two of these co-metabolites were identified by GC/MS as protoillud-6-ene (**2**) and *cis*-dihydroagarofuran (**3**; for mass spectra of **1–3**, see the Supporting Information, Figure S1).^[10,11] For the structure elucidation of **1**, (2,3,4,5,6- $^{13}\text{C}_5$)mevalonolactone was synthesized according to a known procedure (Scheme S1).^[12,13] In this isotopologue of mevalonolactone, all five carbon atoms that are incorporated into terpenes are labeled. The compound was fed to *H. odoratus*, from which [$^{13}\text{C}_{15}$]-**1** was subsequently isolated (16% incorporation; the material was mainly a mixture of unlabeled and completely labeled **1**, see Figure S2A). This allowed for the structure elucidation of **1** by ^{13}C , ^{13}C COSY analysis, which revealed its planar structure (Figure 2).

For the elucidation of the relative configuration, unlabeled **1** was isolated in a yield of 15 mg L^{−1}, and a full set of NMR spectroscopic data, including ^1H , ^{13}C , ^{13}C -DEPT-135, ^1H , ^1H COSY, HSQC, HMBC, and NOESY spectra, was recorded. Comparison of the ^{13}C chemical shifts of **1** (in CDCl_3) to the chemical shifts of previously reported hypodoratoxide (in C_6D_6)^[14] suggested that **1** and hypodoratoxide are identical, which was confirmed by re-examination of the ^{13}C NMR spectrum of **1** in C_6D_6 (Table 1) and comparison of the mass spectra. However, as the ^{13}C , ^{13}C COSY spectrum disagreed with the reported structure **4** of hypodoratoxide,^[14] a structural revision was required. The detected HMBC correlations were in agreement with the structure delineated from the ^{13}C , ^{13}C COSY spectrum (Figure 3), while the overlap of signals from several protons in the ^1H NMR spectrum may have caused misinterpretations of HMBC correlations. As this is a general problem in the structure elucidation of structurally complex natural products, our findings demonstrate the advantage of a ^{13}C , ^{13}C -COSY-based structure elucidation.

The relative configuration of **1** was determined by NOESY spectroscopy (Figure 4). Key correlations were observed between H7 ($\delta = 1.57$ ppm) and H11 ($\delta = 1.25$), placing these on the same face of **1**. This finding was

[*] L. Barra, Prof. Dr. J. S. Dickschat
Kekulé-Institut für Organische Chemie und Biochemie
Rheinische Friedrich-Wilhelms-Universität Bonn
Gerhard-Domagk-Strasse 1, 53121 Bonn (Germany)
E-mail: dickschat@uni-bonn.de

Dr. K. Ibrom
Institut für Organische Chemie, TU Braunschweig
Hagenring 30, 38106 Braunschweig (Germany)

Supporting information for this article is available on the WWW under <http://dx.doi.org/10.1002/anie.201501765>.

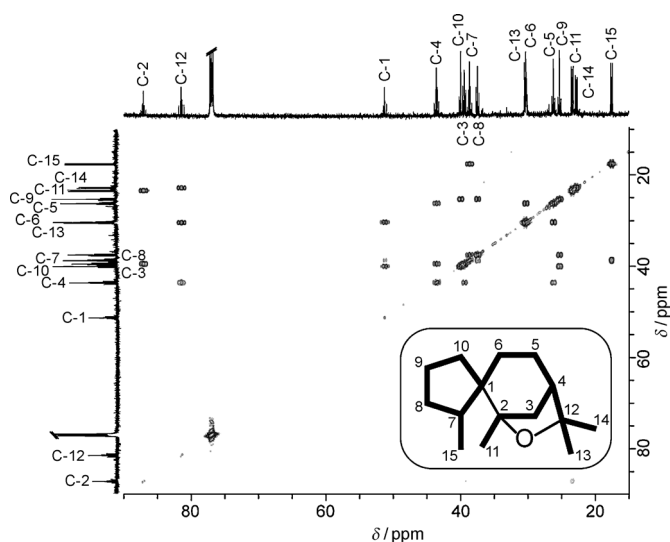


Figure 2. ^{13}C , ^{13}C COSY spectrum of $[\text{C}_{13}]$ -**1** in CDCl_3 . All neighboring carbon atoms along the bold lines of **1** showed cross-peaks, with the exception of the two neighboring quaternary carbon atoms. The reason for the missing signal is that spin relaxation of quaternary carbon atoms is generally slower than for other carbon atoms. The C1–C2 bond was instead inferred from the multiplicities of the signals (Figure S3). An enlarged version of this Figure is presented as Figure S4.

corroborated by a correlation between H6_{eq} ($\delta = 1.47$ ppm) and H15 ($\delta = 1.03$ ppm), which are in similar positions on the opposite face. The equatorial position of H6_{eq} was deduced from a correlation between H6_{ax} ($\delta = 1.65$ ppm) and H14 ($\delta =$

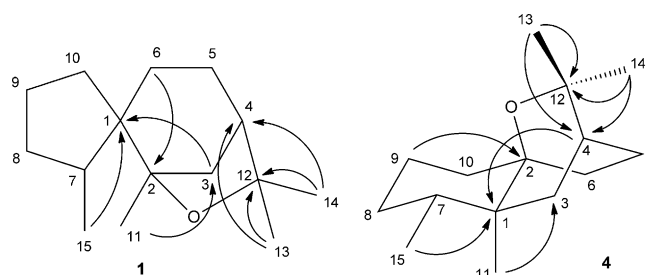


Figure 3. Key HMBC correlations of hypodoratoxide and their interpretation for the revised (**1**) and reported structure (**4**). Carbon atom numbering of **1** is based on IUPAC systematic nomenclature, whereas carbon numbering of **4** followed the reported assignment of ^{13}C NMR signals (Table 1). Note that some of the interpretations of HMBC correlations in the original work involve different hydrogen atoms than in this work (e.g., the correlation H9/C2 is now interpreted as H6/C2 ; the ^1H NMR signals of H9 and H6 overlap).

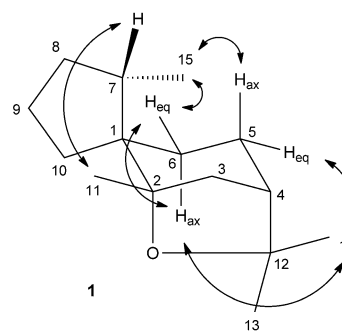


Figure 4. Key NOESY correlations of hypodoratoxide (**1**).

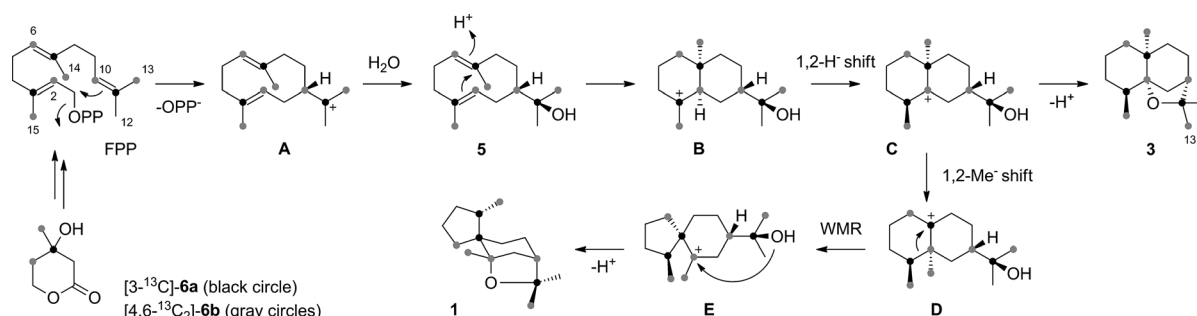
Table 1: ^1H NMR data of **1** and comparison of the ^{13}C NMR data of **1** and hypodoratoxide in C_6D_6 .

$\text{C}^{[a]}$	$^1\text{H}^{[b]}$	$^{13}\text{C}^{[c]}$	$^{13}\text{C}^{[c]}$
	1	1	hypodoratoxide ^[14]
2		86.7 (C_q)	86.7 (C_q)
12		81.3 (C_q)	81.3 (C_q)
1		51.7 (C_q)	51.8 (C_q)
4	1.64, m	44.0 (CH)	44.0 (CH)
10	2.34, dddd, $^2J = 13.6$, $^3J = 7.0$, $^1J = 1.9$, $^4J = 1.9$ 1.05, m	40.5 (CH_2)	40.5 (CH_2)
3	1.75, ddd, $^2J = 11.7$, $^3J = 4.6$, $^4J = 2.5$ 1.62, d, $^2J = 11.8$	39.8 (CH_2)	39.9 (CH_2)
7	1.57, m	38.9 (CH)	38.9 (CH)
8	1.73, m	38.0 (CH_2)	37.9 (CH_2)
	1.08, m		
6	1.65, m	30.9 (CH_2)	30.9 (CH_2)
	1.47, m		
13	1.18, s	30.8 (CH_3)	30.7 (CH_3)
5	1.55, m	26.8 (CH_2)	26.8 (CH_2)
	1.43, m		
9	1.47, m	25.9 (CH_2)	25.8 (CH_2)
	1.23, dddd, $^2J = 12.0$, $^3J = 12.0$, $^1J = 12.0$, $^4J = 7.1$, $^5J = 6.1$		
11	1.25, s	23.9 (CH_3)	23.9 (CH_3)
14	1.29, s	23.2 (CH_3)	23.1 (CH_3)
15	1.03, d, $^3J = 6.8$	17.8 (CH_3)	17.8 (CH_3)

[a] Carbon numbering as shown in Figure 3. [b] Chemical shifts δ in ppm; multiplicity m: s = singlet, d = doublet, m = multiplet; coupling constants nJ refer to couplings via n bonds and are given in Hertz. [c] Chemical shifts δ in ppm; carbon assignments (CH_3 , CH_2 , CH , and C_q) were delineated from a DEPT spectrum.

1.29 ppm). The configuration of the spiro center, that is, the counter-clockwise orientation of the C1, C7, C8, C9, and C10 carbon atoms when looking at **1** as depicted in Figure 4, was evident from a correlation between the axial H5_{ax} atom ($\delta = 1.43$ ppm) and H15 [the equatorial orientation of H5_{eq} ($\delta = 1.55$ ppm) was delineated from its correlation to H14].

A proposed mechanism for the enzymatic conversion of FPP into **1** is shown in Scheme 1. The reaction starts with the cyclization of FPP to the (*E,E*)-germacradienyl cation (**A**), which is attacked by water to yield hedycaryol (**5**). Its protonation initiates a cyclization to cation **B**, which is followed by a 1,2-hydride migration to yield **C**. A subsequent 1,2-methyl shift results in **D**, which gives rise to **1** upon Wagner–Meerwein rearrangement with ring contraction to **E** and intramolecular attack of the



Scheme 1. Biosynthesis of hypodoratoxide (**1**). Gray and black circles indicate ^{13}C -labeled carbon atoms from two individual feeding experiments. PP=diphosphate, WMR=Wagner–Meerwein rearrangement.

hydroxy group at the cationic center with inversion of configuration. The formation of side product **3** is explained by intramolecular attack of the hydroxy group at the cationic center in **C** with retention of configuration (Figure 1). The relative configuration of **3** is in line with that of **1**. Knowledge of the absolute configuration of **3** would point to the absolute configuration of **C**, from which the absolute configuration of **1** could be inferred. Therefore, 18 mg of **3** were isolated from *H. odoratus* with a yield of 3 mg L^{-1} . Its ^{13}C NMR spectroscopic data matched those reported for *cis*-dihydroagarofuran (**3**),^[15] confirming the GC/MS-based identification. The optical activity of isolated (+)-**3** pointed to the absolute configuration that is shown in Scheme 1, which is opposite to that of (–)-**3** from *Prostanthera ovalifolia* (Lamiaceae),^[16] while this is the first report of (+)-**3** from a natural source. Consequently, the absolute configuration of hypodoratoxide is (1*R*,2*S*,4*S*,7*S*)-**1**. This assignment is tentative because a biosynthesis of **1** and **3** by two different terpene cyclases cannot be ruled out.

The proposed cyclization mechanism for **1** was investigated in two feeding experiments with the mevalonolactone isotopologues (3- ^{13}C)-**6a** and (4,6- $^{13}\text{C}_2$)-**6b**.^[12] Feeding of **6a** resulted in the incorporation of the ^{13}C label at the C3, C7, and C11 positions of FPP (68% incorporation, Figure S2B) and allowed for interesting insights into the terpene cyclization. The proposed ring contraction from **D** to **E** was directly evident from the occurrence of doublets for the neighboring labeled carbon atoms C1 and C7 in the ^{13}C NMR spectrum (Figure 5A). Feeding of **6b** gave incorporation of labeling at the C2, C6, C10, C13, C14, and C15 positions of FPP (10% incorporation; see Figure S2C, for the carbon numbering of FPP, see Scheme 1). The ^{13}C NMR spectrum of the terpene cyclization product showed doublets for the neighboring labeled carbon atoms C2 and C11, which is indicative of the 1,2-methyl migration from intermediate **C** to **D** (Figure 5B). The incorporation of labeling almost only at the C13 position (ca. 90% of labeling from C13 of FPP) and only to a low extent at the C14 position of **1** (ca. 10%) revealed a strict stereochemical course for the attack of water at cation **A**. A similar control of the stereochemical course of terpene cyclizations in terms of the fate of the geminal methyl groups of linear terpene precursors was previously observed for other terpene cyclases.^[1,12,17–19]

The strategy of labeling a natural product by feeding of ^{13}C -labeled precursors for structure elucidation by advanced

NMR spectroscopic methods has been applied before in the cases of the diterpene miltiradiene from the lycophyte *Selaginella moellendorffii*,^[20] solwaric acids A and B from the

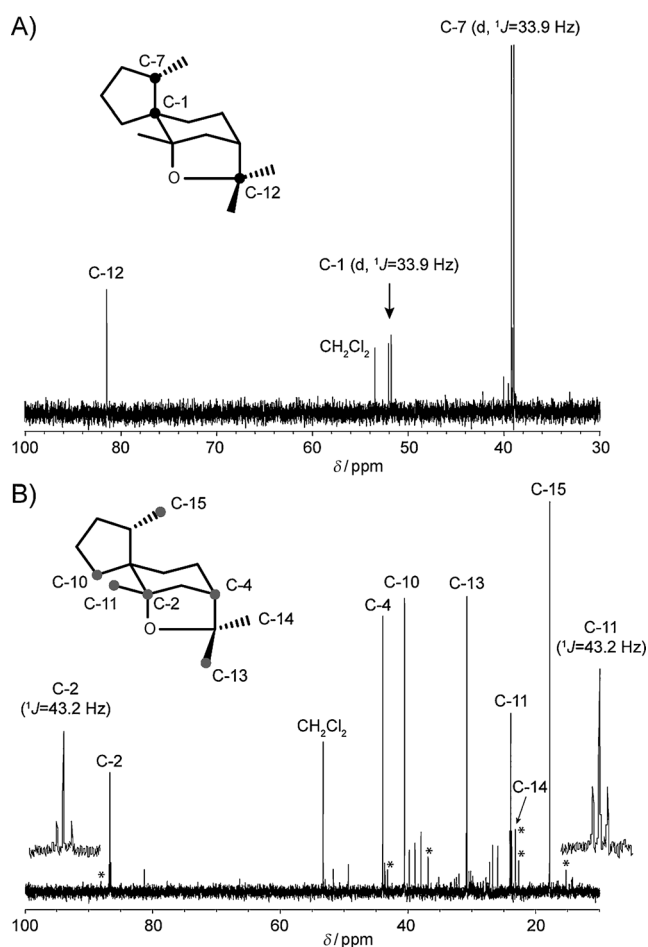


Figure 5. Investigation of the terpene cyclization mechanism by feeding experiments. A) ^{13}C NMR spectrum of [1,7,12- $^{13}\text{C}_3$]-**1** obtained after feeding of (3- ^{13}C)-**6a**. B) ^{13}C NMR spectrum of [2,4,10,11,13,15- $^{13}\text{C}_6$]-**1** obtained after feeding of (4,6- $^{13}\text{C}_2$)-**6b**. The signals for C2 and C11 are also shown in enlarged versions (width: 800%). Some of the additional ^{13}C signals are due to incorporation into the minor product **3** of the hypodoratoxide synthase (labeled with asterisks). The signal at $\delta = 23.1\text{ ppm}$, which was assigned to a minor incorporation into the C14 position of **1**, may also partially account for incorporation into C13 of **3**.

marine actinomycete *Solwaraspora* sp. WMMB-329,^[21] and the polyketide forazoline A from marine *Actinomadura* sp. WMMB-499.^[22] Herein, we provide an example that this strategy makes structure elucidation not only easier, but can also be superior because misinterpretations of HMBC correlations are avoided.

Carefully designed feeding experiments with ¹³C-labeled precursors can give detailed insights into rearrangements of the carbon skeleton during the biosynthesis of a natural product. Whereas rearrangement-induced ¹³C,¹³C couplings have only very rarely been used to prove skeleton rearrangements,^[23] the feeding of multiply ¹³C-labeled precursors, usually (1,2-¹³C₂)acetate, and the loss of ¹³C,¹³C couplings owing to bond cleavages in rearrangements has historically been widely used.^[24] An interesting complementary approach to study the mechanisms of natural-product biosyntheses is the usage of deuterium labeling, as recently performed to follow epimerization reactions in the biosynthesis of non-ribosomal peptides.^[25,26] Another study that combines the usage of ¹³C and ²H labeling in mechanistic investigations of a terpene cyclization has recently been reported from our laboratories.^[27] These and many other previous examples demonstrate how isotopes can successfully be used to solve special problems in natural-products chemistry.

Keywords: biosynthesis · isotopic labeling · NMR spectroscopy · structure elucidation · terpenoids

How to cite: *Angew. Chem. Int. Ed.* **2015**, *54*, 6637–6640
Angew. Chem. **2015**, *127*, 6737–6740

- [1] J. S. Dickschat, *Nat. Prod. Rep.* **2011**, *28*, 1917–1936.
- [2] C. M. Starks, K. Back, J. Chappell, J. P. Noel, *Science* **1997**, *277*, 1815–1820.
- [3] C. A. Lesburg, G. Zhai, D. E. Cane, D. W. Christianson, *Science* **1997**, *277*, 1820–1824.
- [4] M. J. Rynkiewicz, D. E. Cane, D. W. Christianson, *Proc. Natl. Acad. Sci. USA* **2001**, *98*, 13543–13548.
- [5] E. Y. Shishova, L. Di Constanzo, D. E. Cane, D. W. Christianson, *Biochemistry* **2007**, *46*, 1941–1951.
- [6] J. A. Aaron, X. Lin, D. E. Cane, D. W. Christianson, *Biochemistry* **2010**, *49*, 1787–1797.
- [7] M. Köksal, Y. Jin, R. M. Coates, R. Croteau, D. W. Christianson, *Nature* **2011**, *469*, 116–120.
- [8] P. Baer, P. Rabe, C. A. Citron, C. C. de Oliveira Mann, N. Kaufmann, M. Groll, J. S. Dickschat, *ChemBioChem* **2014**, *15*, 213–216.
- [9] P. Baer, P. Rabe, K. Fischer, C. A. Citron, T. A. Klapschinski, M. Groll, J. S. Dickschat, *Angew. Chem. Int. Ed.* **2014**, *53*, 7652–7656; *Angew. Chem.* **2014**, *126*, 7783–7787.
- [10] H. Utsunomiya, J. Kawata, W. Chanoki, N. Shirakawa, M. Miyazawa, *J. Oleo Sci.* **2005**, *54*, 609–612.
- [11] R. P. Adams, *Identification of Essential Oil Components by Gas Chromatography/Mass Spectrometry*, Allured Books, Carol Stream, **2009**.
- [12] L. Barra, B. Schulz, J. S. Dickschat, *ChemBioChem* **2014**, *15*, 2379–2383.
- [13] L. O. Zamir, C.-D. Nguyen, *J. Labelled Compd. Radiopharm.* **1988**, *25*, 1189–1196.
- [14] B. Kühne, H.-P. Hanssen, W.-R. Abraham, V. Wray, *Phytochemistry* **1991**, *30*, 1463–1465.
- [15] J.-F. Cavalli, F. Tomi, A.-F. Bernardini, J. Casanova, *Magn. Reson. Chem.* **2004**, *42*, 709–711.
- [16] I. A. Southwell, D. J. Tucker, *Phytochemistry* **1993**, *33*, 857–862.
- [17] X. Lin, D. E. Cane, *J. Am. Chem. Soc.* **2009**, *131*, 6332–6333.
- [18] N. L. Brock, S. R. Ravella, S. Schulz, J. S. Dickschat, *Angew. Chem. Int. Ed.* **2013**, *52*, 2100–2104; *Angew. Chem.* **2013**, *125*, 2154–2158.
- [19] C. A. Citron, N. L. Brock, B. Tudzynski, J. S. Dickschat, *Chem. Commun.* **2014**, *50*, 5224–5226.
- [20] Y. Sugai, Y. Ueno, K. Hayashi, S. Oogami, T. Toyomasu, S. Matsumoto, M. Natsume, H. Nozaki, H. Kawaide, *J. Biol. Chem.* **2011**, *286*, 42840–42847.
- [21] G. A. Ellis, T. P. Wyche, C. G. Fry, D. R. Braun, T. S. Bugni, *Mar. Drugs* **2014**, *12*, 1013–1022.
- [22] T. P. Wyche, J. S. Piotrowski, Y. Hou, D. Braun, R. Deshpande, S. McIlwain, I. M. Ong, C. L. Myers, I. A. Guzei, W. M. Westler, D. R. Andes, T. S. Bugni, *Angew. Chem. Int. Ed.* **2014**, *53*, 11583–11586; *Angew. Chem.* **2014**, *126*, 11767–11770.
- [23] A. P. W. Bradshaw, J. R. Hanson, M. Sivers, *J. Chem. Soc. Chem. Commun.* **1977**, 819a.
- [24] T. J. Simpson, *Top. Curr. Chem.* **1998**, *195*, 1–48.
- [25] H. B. Bode, D. Reimer, S. W. Fuchs, F. Kirchner, C. Dauth, C. Kegler, W. Lorenzen, A. O. Brachmann, P. Grün, *Chem. Eur. J.* **2012**, *18*, 2342–2348.
- [26] B. Morinaka, A. L. Vagstad, M. J. Helf, M. Gugger, C. Kegler, M. F. Freeman, H. B. Bode, J. Piel, *Angew. Chem. Int. Ed.* **2014**, *53*, 8503–8507; *Angew. Chem.* **2014**, *126*, 8643–8647.
- [27] P. Rabe, K. A. K. Pahirulzaman, J. S. Dickschat, *Angew. Chem. Int. Ed.* **2015**, DOI: 10.1002/anie.201501119; *Angew. Chem.* **2015**, DOI: 10.1002/ange.201501119.

Received: February 24, 2015

Published online: April 15, 2015